



Boundary control, quiet boundaries, super-stability and super-instability

Firdaus E. Udwardia

*Aerospace and Mechanical Engineering, Civil Engineering, Mathematics,
and Information and Operations Management,
University of Southern California, 430 K Olin Hall, Los Angeles, CA 90089-1453, USA*

Abstract

This paper deals with the boundary feedback control of a bar undergoing axial vibrations. The feedback force is applied to one end of the bar and it is proportional to its velocity. The problem is of fundamental interest in control theory, structural dynamics, and the development of ‘quiet boundaries’ in fields like earthquake engineering and computational mechanics. The system is not self-adjoint and exhibits a variety of interesting behaviors which are explained through a combination of several inter-twined strands of thought using mathematics, physical interpretations, and numerical simulations. Besides providing a rigorous mathematical solution to the problem, the paper explains the physical origin of super-stable behavior, introduces the new concept of super-unstable behavior, and points out that these regimes of behavior are intricately connected with the continuum model that is used. It is shown that any finite-dimensional approximation of the system, no matter how finely discretized, can not qualitatively depict superstable behavior.

© 2004 Elsevier Inc. All rights reserved.

E-mail address: fudwdia@usc.edu

1. Introduction

The use of boundary control of distributed parameter systems is becoming more and more important in technological applications in numerous fields ranging from the control of structural and mechanical systems to chemical and environmental process control [1–4]. This paper explores the dynamics and control of a simple system modeled by the one dimensional wave equation, and shows some interesting characteristics which are bestowed on the system's behavior by virtue of the boundary conditions imposed at its ends. These boundary conditions are of some significant interest for they appear in a natural manner in devising stable controllers for distributed vibrating systems as well as in the problem of generating 'quiet boundaries' in systems where the reflection of waves from the boundaries of a medium need to be reduced, or perhaps even completely eliminated.

Unfortunately, from a mathematical standpoint the system is not self-adjoint and hence the usual methods for its analysis need to be used with some care. We shall use a combination of physical interpretations along with a rigorous analysis of this problem to describe the characteristics of the system's response. Along the way we shall encounter multiple, and connected, strands of thinking used by mechanicians, control theorists, and mathematicians.

We consider the problem of the axial vibrations of an elastic bar of unit length and constant cross sectional area, A_0 , which is fixed at one end and is subjected to a force that is proportional to its velocity at the other. The equation describing its motion is given by

$$\rho \frac{\partial^2 u(x, t)}{\partial t^2} = EA_0 \frac{\partial^2 u(x, t)}{\partial x^2}, \quad 0 < x < 1, \quad (1)$$

with the boundary conditions

$$u(0, t) = 0, \quad \text{and} \quad EA_0 \frac{\partial u(1, t)}{\partial x} = -\eta \frac{\partial u(1, t)}{\partial t} \quad (2)$$

and the initial conditions

$$u(x, 0) = f(x), \quad \text{and} \quad \frac{\partial u(x, 0)}{\partial t} = g(x) \quad \text{when} \quad 0 < x < 1. \quad (3)$$

Here ρ is the density of the bar per unit length, E is its modulus of elasticity, and the parameter η is a real number. Denoting the wave speed in the bar by $c = \sqrt{EA_0/\rho} > 0$, and the dimensionless parameter $\alpha = \frac{EA_0}{\eta c}$, we can rewrite Eqs. (1)–(3) as

$$\frac{\partial^2 u(x, t)}{\partial t^2} = c^2 \frac{\partial^2 u(x, t)}{\partial x^2}, \quad 0 < x < 1, \quad (1a)$$

$$u(0, t) = 0, \quad \text{and} \quad \alpha c \frac{\partial u(1, t)}{\partial x} = -\frac{\partial u(1, t)}{\partial t}, \quad \text{and} \tag{2a}$$

$$u(x, 0) = f(x), \quad \text{and} \quad \frac{\partial u(x, 0)}{\partial t} = g(x), \quad \text{when } 0 < x < 1. \tag{3a}$$

We note that the system is *not* self-adjoint, but still begin by considering the ansatz

$$u(x, t) = \exp(i\omega t)v(x), \tag{4}$$

where we shall, of course, be interested in only the real part of the right hand side of Eq. (4). Eq. (1a) then becomes

$$\frac{d^2v}{dx^2} + (\omega/c)^2v = 0, \tag{5}$$

and the boundary conditions can be expressed as

$$v(0) = 0, \quad \text{and} \quad \alpha c \frac{dv(1)}{dx} = -i\omega v(1). \tag{6}$$

The solution of Eq. (5), by virtue of the boundary condition at $x = 0$, is given by

$$v(x) = A \sin\left(\frac{\omega x}{c}\right), \tag{7}$$

where A is an arbitrary (complex) constant. The boundary condition at $x = 1$ yields the relation

$$\tan\left(\frac{\omega}{c}\right) = i\alpha \tag{8}$$

pointing out that for our ansatz to be valid, the value of ω must be restricted to one of those that satisfy Eq. (8). Denoting the complex variable $z = p + iq = \omega/c$, Eq. (8) can be rewritten as

$$e^{2iz} = e^{2ip-2q} = \frac{1 - \alpha}{1 + \alpha}. \tag{9}$$

It is convenient to consider the following three cases:

(1) $|\alpha| < 1$, so that the solution of Eq. (9) is

$$p_n = n\pi, \quad n = 0, 1, 2, \dots, \quad \text{and} \quad q_0(\alpha) = -\frac{1}{2} \ln \left| \frac{1 - \alpha}{1 + \alpha} \right| \tag{10}$$

and

$$\omega_n = p_n c + iq_0(\alpha)c = n\pi c - \frac{ic}{2} \ln \left| \frac{1 - \alpha}{1 + \alpha} \right|, \quad n = 0, 1, 2, \dots \tag{11}$$

(2) $|\alpha| > 1$, so that the solution of Eq. (8) is

$$p_n = \frac{2n + 1}{2} \pi, \quad n = 0, 1, 2, \dots, \quad \text{and} \quad q_0(\alpha) = -\frac{1}{2} \ln \left| \frac{1 - \alpha}{1 + \alpha} \right|, \tag{12}$$

and

$$\omega_n = p_n c + i q_0(\alpha) c = \frac{2n + 1}{2} \pi c - \frac{ic}{2} \ln \left| \frac{1 - \alpha}{1 + \alpha} \right|, \quad n = 0, 1, 2, \dots \tag{13}$$

(3) $\alpha = \pm 1$, so that the solution of Eq. (8) is now

$$p = \text{arbitrary}, \quad \text{and} \quad q_0 = \pm \infty. \tag{14}$$

It is informative to see the manner in which the ω_n 's vary with the dimensionless parameter α by considering the real and imaginary parts of $\tan(z) = \tan(p + iq)$. This is particularly important to explain the case when $\alpha = 1$, which, as we shall see later, has considerable physical significance.

For,

$$\tan(z) = \frac{\sin 2p}{\cos 2p + \cosh 2q} + i \frac{\sinh 2q}{\cos 2p + \cosh 2q} \tag{15}$$

so that condition (9) requires

$$\sin 2p = 0, \quad \text{or} \quad 2p = n\pi, \quad n = 0, 1, 2, \dots \tag{16}$$

and $q = q_0(\alpha)$ must satisfy the relation

$$\frac{\sinh 2q}{\cosh 2q \pm 1} = \alpha. \tag{17}$$

Fig. 1 shows the two branches of the function on the left hand side of Eq. (17). The figure shows that for $|\alpha| > 1$, the value of the root, $q_0(\alpha)$, in Eq. (17) is obtained using the negative sign in Eq. (17); for $|\alpha| < 1$, the root $q_0(\alpha)$ is obtained using the positive sign in (17). We also see that for $\alpha > 0$, the value of $q_0 > 0$; for $\alpha < 0$, the value of $q_0 < 0$.

The function $u(x, t)$ corresponding to our ansatz defined in Eq. (4) is then given by

$$u_n(x, t) = A_n e^{-q_0(\alpha)ct} e^{in\pi ct} \sin\{n\pi x + iq_0(\alpha)x\}, \quad n = 0, 1, 2, \dots \quad \text{for } |\alpha| < 1, \tag{18}$$

and

$$u_n(x, t) = A_n e^{-q_0(\alpha)ct} e^{i\left(\frac{2n+1}{2}\right)\pi ct} \sin\left(\frac{2n+1}{2} \pi x + iq_0(\alpha)x\right), \tag{19}$$

$$n = 0, 1, 2, \dots \quad \text{for } |\alpha| > 1.$$

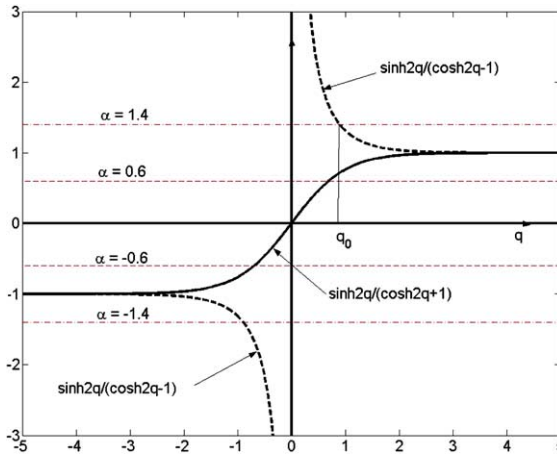


Fig. 1. The two branches of the function on the left hand side of Eq. (17) are shown. The roots $q_0(\alpha)$ of Eq. (17) for different values of $\alpha = -1.4, -0.6, 0.6$ and 1.4 are the intersections of the horizontal lines with the corresponding branches of the curves. As $\alpha \rightarrow \pm 1, q_0 \rightarrow \pm\infty$.

From here on, for brevity, we shall suppress showing the explicit dependence of q_0 on α . Since we are interested only in the real part of $u(x,t)$, we obtain the response to our original problem (1a)–(3a), as per our ansatz, to be

$$u_n(x, t) = B_n e^{-q_0(x+ct)} \cos[p_n(x + ct) + \varphi_n] - B_n e^{-q_0(ct-x)} \cos[p_n(x - ct) - \varphi_n], \tag{20}$$

where we have denoted the complex coefficient, $A_n = 2B_n \exp i(\varphi_n + \frac{\pi}{2})$, with B_n a real number. The values of p_n in Eq. (20) are given by Eqs. (10) and (12) for $|\alpha| < 1$ and $|\alpha| > 1$ respectively. We can also write relation (20) in another form, which will be useful to us later on, as

$$u_n(x, t) = C_n [e^{-q_0(x+ct)} \cos p_n(x + ct) - e^{-q_0(ct-x)} \cos p_n(ct - x)] + D_n [e^{-q_0(ct-x)} \sin p_n(ct - x) - e^{-q_0(x+ct)} \sin p_n(x + ct)] \tag{21}$$

where the constants C_n and D_n are real.

When $\alpha > 0$, as stated before, $q_0 > 0$, and relation (20) shows that if our ansatz is correct, the response $u_n(x,t)$ must be exponentially damped in time. Relation (21) indicates that $u_n(x,t)$ can also be thought of as a set of exponentially damped traveling waves; and, the damping factor, $q_0(\alpha)$, does *not* depend on the value of the mode number, n .

The situation when $|\alpha| = 1$ can be seen from Fig. 1. The two branches tend to ± 1 as $\alpha \rightarrow \pm 1$, and accordingly the root $q_0 \rightarrow \infty \pm$; the exponent in relations (20) and (21) goes to $\mp \infty$. And so we find that for $\alpha = +1$, our assumed solution seems to vanish for $t > x/c$ (because $q_0 = \infty$), and for $\alpha = -1$ it explodes at

$t = 0_+$! There appears to be a vanishing of the amplitude of $u(x,t)$ in one case, and an ‘instantaneous’ explosion of its amplitude in the other. We shall need to refine these ideas as we go along, for we notice from the two members in (20) that it is their difference that is involved. We note that when $\alpha = 1$, the boundary condition (2a) reads

$$c \frac{\partial u(1,t)}{\partial x} = - \frac{\partial u(1,t)}{\partial t}. \quad (22)$$

Before we move on we must note that while we might be tempted to use the functions $u_n(x,t)$ as ‘eigenfunctions,’ the system described by the Eqs. (5) and (6) is not self-adjoint and therefore such a direct approach could be invalid. Indeed we shall show that is the case when $\alpha = 1$.

2. Boundary control and stability

The boundary condition (2) can be viewed as a control force that is applied to the bar at its boundary $x = 1$, the force being proportional to the velocity at this boundary. The effect of the boundary condition (2), or (2a), on the response of the bar can be seen by considering the energy $E(t)$ of the vibrating system given by

$$E(t) = \frac{1}{2} \int_0^1 c^2 \left(\frac{\partial u}{\partial x} \right)^2 dx + \frac{1}{2} \int_0^1 \left(\frac{\partial u}{\partial t} \right)^2 dx. \quad (23)$$

The function $E(t)$ is positive definite, and its derivative with respect to time is given by

$$\begin{aligned} \frac{dE}{dt} &= c^2 \int_0^1 \frac{\partial u}{\partial x} \frac{\partial^2 u}{\partial x \partial t} dx + \int_0^1 \frac{\partial u}{\partial t} \frac{\partial^2 u}{\partial t^2} = c^2 \frac{\partial u}{\partial x} \frac{\partial u}{\partial t} \Big|_0^1 + \int_0^1 \frac{\partial u}{\partial t} \left[\frac{\partial^2 u}{\partial t^2} - \frac{\partial^2 u}{\partial x^2} \right] \\ &= c^2 \frac{\partial u(1,t)}{\partial x} \frac{\partial u(1,t)}{\partial t} = -\alpha c^3 \left(\frac{\partial u(1,t)}{\partial x} \right)^2, \end{aligned} \quad (24)$$

where we have used Eq. (1a) in the third equality and the boundary conditions (2a) in the fourth. Thus, using $E(t)$ as a Lyapunov function, for $\alpha \geq 0$ we have Lyapunov stability; and for $\alpha > 0$, we suspect asymptotic Lyapunov stability. Indeed, the manifold on which $\dot{E}(t)$ is semi-positive definite is $u(x,t) \equiv 0, u_t(x,t) \equiv 0$ so that zero is asymptotically stable (see Ref. [6] also). On the other hand for $\alpha < 0$, the energy of the system keeps increasing and we expect the boundary control to be unstable. This appears to agree with our conclusion in the previous section where we found that the ansatz $u(x,t) = e^{i\omega t} v(x)$ will lead to exponentially decreasing amplitudes (over long enough times) for $\alpha > 0$, and exponentially increasing ones for $\alpha < 0$. The simple energy analysis provided above does not, however, signal any special type of response when $\alpha = \pm 1$.

We shall show after we determine the system’s response that for these values of α the system does indeed show peculiar behavior.

3. Response of the system with boundary control

As stated before, our boundary value problem is not self-adjoint and therefore direct appeal to methods using eigenfunction expansions need to be carried out with some care. Having been assured of stability for $\alpha \geq 0$, in this section we will concern ourselves primarily with positive values of α , for we desire our control to be stable. Taking the Laplace Transform of Eq. (1a) with respect to time, t , we get

$$\frac{d^2U(x,s)}{dx^2} - \frac{s^2}{c^2}U(x,s) = -\frac{sf(x) + g(x)}{c^2} := -\frac{F(x,s)}{c^2}, \tag{25a}$$

$$U(0,s) = 0, \text{ and } \alpha c \frac{dU(1,s)}{dx} = f(1) - sU(1,s), \tag{25b}$$

where we have denoted the Laplace Transform of $u(x,t)$ by $U(x,s)$. In what follows we shall take the initial condition to be such that $f(1) = 0$. In fact, we shall find it convenient to define the functions $f(x)$ and $g(x)$ to be zero outside the interval $(0,1)$. We note that the function $F(x,s)$ defined in Eq. (25a) is analytic in the complex variable s .

The Green’s function for the resulting two-point boundary value problem described by Eqs. (25a) and (25b) can be obtained as

$$G(x, \xi; s) = \begin{cases} G_1(x, \xi; s) = \frac{c}{s\gamma_1} [\gamma_2 \sinh(\frac{s}{c}x) - \gamma_1 \cosh(\frac{s}{c}x)] \sinh(\frac{s}{c}\xi) & \text{for } \xi \leq x, \\ G_2(x, \xi; s) = \frac{c}{s\gamma_1} [\gamma_2 \sinh(\frac{s}{c}\xi) - \gamma_1 \cosh(\frac{s}{c}\xi)] \sinh(\frac{s}{c}x) & \text{for } \xi \geq x, \end{cases} \tag{26}$$

where we have denoted

$$\gamma_1(s; \alpha) = \sinh \frac{s}{c} + \alpha \cosh \frac{s}{c}, \tag{27}$$

and

$$\gamma_2(s; \alpha) = \alpha \sinh \frac{s}{c} + \cosh \frac{s}{c}. \tag{28}$$

This yields

$$U(x,s) = -\frac{1}{c^2} \int_0^x G_1(x, \xi; s)F(\xi,s) d\xi - \frac{1}{c^2} \int_x^1 G_2(x, \xi; s)F(\xi,s) d\xi. \tag{29}$$

We observe from relations (26) and (29) that the function $U(x,s)$ (and $G(x,\xi;s)$) has poles, only at $s = s_n$, which are the roots of the equation $\gamma_1 = 0$, and are given by

$$\tanh \frac{s_n}{c} = -\alpha. \tag{30}$$

This is, of course, the same as Eq. (8) were we to replace s_n by $i\omega_n$ in it. Hence the roots of Eq. (30) are simply given by

$$s_n = -q_0c + ip_n c, \quad n = 0, \pm 1, \pm 2, \dots, \tag{31}$$

where q_0 is given by Eq. (10), and the values of p_n depend on the range of the parameter α , as before (see Eqs. (10)–(14)). There is no pole at $s = 0$.

Using relation (26), we can now simplify Eq. (29) to read

$$U(x,s) = -\frac{1}{c} \int_0^x \left[\frac{\gamma_2(s;\alpha) \sinh \frac{sx}{c} - \gamma_1(s;\alpha) \cosh \frac{sx}{c}}{\gamma_1(s;\alpha)} \right] \left[\sinh \frac{s\xi}{c} \right] \frac{F(\xi,s)}{s} d\xi - \frac{1}{c} \int_x^1 \left[\frac{\gamma_2(s;\alpha) \sinh \frac{s\xi}{c} - \gamma_1(s;\alpha) \cosh \frac{s\xi}{c}}{\gamma_1(s;\alpha)} \right] \left[\sinh \frac{sx}{c} \right] \frac{F(\xi,s)}{s} d\xi. \tag{32}$$

The inverse transform of Eq. (32) then gives the response of the system described by Eqs. (1a)–(3a).

We note that for $\alpha = 1$, relation (17) gives $q_0 = \infty$, and all the poles, s_n , given by Eq. (31), lie in the left half complex plane s -plane, their abscissa being at $-\infty$! In fact, when $\alpha = 1$, we have by relations (27) and (28) that $\gamma_1(s;1) = \gamma_2(s;1)$. Hence the Green’s function given by Eq. (26) reduces to

$$G(x,\xi;s) = \begin{cases} G_1(x,\xi;s) = \frac{c}{s} \left[\sinh \left(\frac{\xi}{c} x \right) - \cosh \left(\frac{\xi}{c} x \right) \right] \sinh \left(\frac{\xi}{c} \xi \right), & \text{for } \xi \leq x, \\ G_2(x,\xi;s) = \frac{c}{s} \left[\sinh \left(\frac{\xi}{c} \xi \right) - \cosh \left(\frac{\xi}{c} \xi \right) \right] \sinh \left(\frac{\xi}{c} x \right), & \text{for } \xi \geq x, \end{cases} \tag{33}$$

which, we note, is an entire function in the complex s -plane.

The Green’s function being entire says that *all values* of s lie in the resolvent set of the operator and hence there are no (finite) points in the spectrum of the operator. *And since the spectrum is empty, the system then has no finite eigenvalues and hence no eigenfunctions!* This remarkable behavior of our boundary controlled system when $\alpha = 1$ can best be understood by looking at the time response of the system. The Laplace transform given in Eq. (32) now simplifies to

$$U(x,s) = -\frac{1}{c} \int_0^x \left[\sinh \frac{sx}{c} - \cosh \frac{sx}{c} \right] \left[\sinh \frac{s\xi}{c} \right] \frac{F(\xi,s)}{s} d\xi - \frac{1}{c} \int_x^1 \left[\sinh \frac{s\xi}{c} - \cosh \frac{s\xi}{c} \right] \left[\sinh \frac{sx}{c} \right] \frac{F(\xi,s)}{s} d\xi. \tag{34}$$

The inverse transform of $U(x,s)$ given in Eq. (34) can now be trivially obtained as

$$u(x,t)|_{x=1} = \frac{1}{2} \{f(x-ct) + f(x+ct)\} + \frac{1}{2} \int_0^t \{g(x+c\tau) + g(x-c\tau)\} d\tau - \frac{1}{2} \left\{ f(ct-x) + \int_0^t g(c\tau-x) d\tau \right\}, \tag{35}$$

where we define the functions $f(x)$ and $g(x)$ to be zero outside the interval $(0,1)$. Eq. (35) shows that when $\alpha = 1$, the response of the bar, $u(x,t)$, is made up of traveling waves. The terms in the bracket on the second line of Eq. (35) are contributions from the reflection of the leftward traveling waves from the boundary at $x = 0$. The negative sign preceding this bracket indicates that at this fixed boundary, a tensile wave is reflected as a compressive wave, and vice-versa. We next consider a peculiarity of this solution.

Consider *any* fixed point on the bar located at $x = x_0$ and any time $t_0 \geq \frac{2}{c}$. Notice that $\frac{2}{c}$ is simply twice the time taken for a wave moving at speed c to traverse the length of the bar, which has unit length. When $\alpha = 1$, the response, $u(x_0,t_0)$, can be found by evaluating each of the terms given in Eq. (35). Since $t_0 \geq \frac{2}{c}$,

$$f(x_0 - ct_0) = f(x_0 + ct_0) = f(ct - x_0) = 0, \tag{36}$$

and

$$\int_0^{t_0} \{g(x_0 + c\tau) + g(x_0 - c\tau)\} d\tau = \int_0^{t_0} g(c\tau - x_0) d\tau = \int_0^1 g(x) dx. \tag{37}$$

Hence, using Eq. (35), we find that

$$u(x,t)|_{x=1} \equiv 0 \text{ for all } t \geq \frac{2}{c}. \tag{38}$$

Every point of the bar comes to rest in *finite* time! We shall come back to this somewhat unusual behavior that is engendered by the boundary controlled system when $\alpha = 1$.

It is also interesting to consider the Green’s function when $\alpha = -1$. Relation (17) now gives $q_0 = -\infty$, and so all the poles, s_n , which are given by Eq. (31), lie, as it were, in the right-half of the complex s -plane, their abscissas being located at ∞ ! From relations (27) and (28) we observe that $\gamma_1(s;-1) = -\gamma_2(s;-1)$. Hence, for $\alpha = -1$, the Green’s function given by Eq. (26) reduces to

$$G(x, \xi; s) = \begin{cases} G_1(x, \xi; s) = -\frac{c}{s} \left[\sinh\left(\frac{s}{c}x\right) + \cosh\left(\frac{s}{c}x\right) \right] \sinh\left(\frac{s}{c}\xi\right), & \text{for } \xi \leq x \\ G_2(x, \xi; s) = -\frac{c}{s} \left[\sinh\left(\frac{s}{c}\xi\right) + \cosh\left(\frac{s}{c}\xi\right) \right] \sinh\left(\frac{s}{c}x\right), & \text{for } \xi \geq x \end{cases} \tag{39}$$

which, like the Green’s function that we obtained for $\alpha = 1$ in Eq. (33), is also an entire function in the complex s -plane! And, like for $\alpha = 1$, there are no eigenvalues or eigenfunctions when $\alpha = -1$. The development of this result is straight-forward and elementary; Datko [5] has used finite Laplace transforms, and the fact that they are entire functions in the complex plane, to arrive at a similar result, while Chen [6] has used energy decay rates to look at stabilization for systems that satisfy his so-called D-conditions.

However, as we shall see in the next section, this mathematical likeness is a bit misleading since the response of the system when $\alpha = -1$ is vastly dissimilar from that when $\alpha = 1$. As shown in Fig. 1, the difference lies in the fact that when $\alpha = 1$ the Green’s function is entire because all its poles are, as it were, in the left half s -plane with their abscissas being at $-\infty$, while when $\alpha = -1$ all the poles of the Green’s function are, as it were, in the right half s -plane their abscissas being at $+\infty$! It is this difference that causes the system to be super-stable in the former case, and super-unstable in the latter.

Having dealt with the case $|\alpha| = 1$, let us go back to the inversion of $U(x, s)$ for $|\alpha| \neq 1$. Using Eq. (32) we obtain

$$u(x, t) = L^{-1}[U(x, s)], \tag{40}$$

where L^{-1} denotes the inverse Laplace Transform.

Before finding the inverse Laplace transform described by the first term on the right hand side of Eq. (40), we note from the definitions of $\gamma_1(s; \alpha)$ and $\gamma_2(s; \alpha)$ given in Eqs. (27) and (28) that

$$\gamma_2(s; \alpha) = c \frac{d\gamma_1(s; \alpha)}{ds}. \tag{41}$$

Since the zeros of $\gamma_1(s; \alpha)$ for $|\alpha| \neq 1$ are simple, $u(x, t)$ becomes

$$u(x, t) = - \sum_{n=-\infty}^{\infty} e^{s_n t} \frac{\sinh \frac{s_n}{c} x}{s_n} \int_0^1 \sinh \left(\frac{s_n}{c} \xi \right) F(\xi, s_n) d\xi \tag{42}$$

In the above equation we have used relation (41) to determine the residues at the poles $s_n = -q_0 c + ip_n c$ where q_0 and p_n are given by relations (10) and (12). After some algebra, Eq. (42) can be rewritten in a more understandable, though less compact, form as

$$\begin{aligned} u(x, t) = & \sum_{n=0}^{\infty} (C_n^{(1)} + C_n^{(2)}) [e^{-q_0(x+ct)} \cos p_n(x+ct) - e^{-q_0(ct-x)} \cos p_n(ct-x)] \\ & + \sum_{n=0}^{\infty} (D_n^{(1)} + D_n^{(2)}) [e^{-q_0(ct-x)} \sin p_n(ct-x) - e^{-q_0(x+ct)} \sin p_n(x+ct)], \end{aligned} \tag{43}$$

where

$$C_n^{(1)} = \frac{1}{2} \int_0^1 [e^{q_0 \xi} - e^{-q_0 \xi}] \cos p_n \xi f(\xi) d\xi, \tag{44}$$

$$D_n^{(1)} = -\frac{1}{2} \int_0^1 [e^{q_0 \xi} + e^{-q_0 \xi}] \sin p_n \xi f(\xi) d\xi, \tag{45}$$

$$C_n = \frac{1}{2} \int_0^1 [e^{q_0 \xi} - e^{-q_0 \xi}] \cos p_n \xi g(\xi) d\xi, \tag{46}$$

$$D_n = -\frac{1}{2} \int_0^1 [e^{q_0 \xi} + e^{-q_0 \xi}] \sin p_n \xi g(\xi) d\xi, \tag{47}$$

$$C_n^{(2)} = \frac{C_n \cos \varphi_n + D_n \sin \varphi_n}{|s_n|}, \quad D_n^{(2)} = \frac{D_n \cos \varphi_n - C_n \sin \varphi_n}{|s_n|} \tag{48}$$

and φ_n is the phase angle of the pole

$$s_n = -q_0 c + i p_n c = |s_n| \exp(i\varphi_n). \tag{49}$$

As before, the values taken by p_n are given by relations (10) and (12), depending on the range of in which the parameter α lies. When $|\alpha < 1|$, $s_0 = -q_0 c$, and the values of $C_0^{(i)}$ and $D_0^{(i)}$, $i = 1, 2$, must then be replaced by half those found from relations (44) and (48). We have now obtained the complete solution of our boundary control problem.

Comparing the form of Eq. (43) and the $u_n(x,t)$ obtained in Eq. (21) tells us that $u(x,t)$ is just what we might have expected our naïve initial ansatz to have provided us with for eigenfunctions of the system, the response $u(x,t)$ being nothing other than an expansion in terms of these functions! Each term in the expansion (46) is an exponentially decaying traveling wave that represents the continued reflections of the traveling waves from the boundaries.

Relations (42)–(49) inform us that the response, $u(x,t)$, of the our boundary controlled system which is described by Eqs. 1a,2a,3a can still be expressed for $|\alpha| \neq 1$ solely as a weighted sum of the functions $u_n(x,t)$ that we got in Eq. (21). To understand the disappearance of the transient solution $u(x,t)|_{\alpha=1}$ after a time greater than $\frac{2}{c}$, we now turn to the wave interpretation of this boundary-controlled system.

4. Quiet boundaries and eigenvalues

The problem of interpreting the solution that we have found of our system that is described by Eqs. (1a)–(3a) revolves around the boundary condition at $x = 1$. It is this boundary condition that causes the problem to become non-self-adjoint, and so to understand the behavior of the solution it is worthwhile

looking at the manner in which this boundary alters the waves that travel along the bar. In order to do this and focus upon the effect of this right hand boundary, let us first imagine that the left-hand boundary of the bar is moved from $x = 0$ to $x = -\infty$.

The medium of our semi-infinite bar is thus described by relation (1a), namely, $u_{tt} = c^2 u_{xx}$, and this medium can sustain a response given as $u(x,t) = u_1(x - ct) + u_2(x + ct)$. Thus the medium supports waves that can travel to the right and the left, with a speed c . We expand the rightward traveling wave (the leftward traveling wave moves towards $x = -\infty$ since the bar is semi-infinite), as $u_1(x - ct) = \int_{-\infty}^{\infty} A(\omega) e^{i(kx - \omega t)}$, and consider one harmonic component of it, namely, $v_1(x,t) = A e^{i(kx - \omega t)}$. This component has an amplitude A , wave number k , and frequency ω , so that $\omega = kc$. Upon meeting the right-hand boundary at $x = 1$, it undergoes, in general, a modification. For, the total wave field,

$$v(x,t) = v_1(x,t) + v_R(x,t) \quad (50)$$

is now required to satisfy the boundary condition thereat, namely,

$$\alpha c \frac{\partial v(1,t)}{\partial x} = - \frac{\partial v(1,t)}{\partial t}. \quad (51)$$

This modification described by Eq. (51), however, can only consist of adding to our right-traveling wave, $v_1(x,t)$, another ‘reflected’ left-traveling wave $v_R = A R e^{-i(kx + \omega t)}$, where R is the reflection coefficient to be determined by ensuring that relation (51) is satisfied. This requires

$$R = - \frac{1 - \alpha}{1 + \alpha} e^{2ik}. \quad (52)$$

Several observations can be drawn from relation (52).

Observation 1: When $\alpha = 1$, the reflection coefficient is zero, and this is true for all wave numbers! The reflected wave, v_R , has zero amplitude, and the total wave field, $v(x,t)$, remains, by (52), the same as $v_1(x,t)$. Such a boundary may be called a *quiet boundary*, for it does not disclose its presence by causing any modification to the wave that impinges on it. And since the medium stops at $x = 1$, the wave seems to ‘disappear’ on the right, past this boundary at $x = 1$.

Observation 2: We can now bring our left boundary of the bar back (from $x = -\infty$) to $x = 0$. We can easily find that the boundary condition $v(0,t) = 0$ requires that any leftward traveling wave be reflected from this boundary with the reflection coefficient R of -1 . There is no energy lost in this reflection process at $x = 0$.

Observation 3: We can interpret the response of the system described by Eqs. (1a)–(3a) as being fundamentally governed by the operator $u_{tt} = c^2 u_{xx}$ that is valid throughout the domain (0,1). The ‘boundary conditions’ serve to modify this response. Often they cause reflections of the waves that impinge upon

them. This may lead to the setting up of interference patterns, and standing waves, which are often associated with mode shapes (eigenmodes) and frequencies of vibration (eigenfrequencies).

Observation 4: When $\alpha = 1$, the right boundary condition generates no reflections, no interference patterns, no standing waves, and hence the response of the system cannot be expressed in terms of eigenvalues and eigenfunctions. Another way of saying this is that the Green's function is analytic, for all its poles (eigenvalues) are in the left half s -plane and at an abscissa of $-\infty$, as we saw before. Recall that our naïve initial ansatz gave exponential damping in time, with the exponent being $-\infty$.

Observation 5: When $\alpha = 1$, energy is irretrievably 'leaked' out of the system because the rightward traveling waves simply 'disappear' beyond $x = 1$, and nothing is reflected back from the right hand boundary. These rightward traveling waves continue onwards as though the boundary were completely 'transparent' to them. The boundary acts as a 'sink' of energy and drains the energy out of the vibrating system, reflecting none back.

Observation 6: For values of $\alpha \neq 1$, this transparency is lost. There is a continued reflection of the wave from the right hand boundary and this is primarily captured by the expression given in Eq. (43). When $\alpha > 1$, the reflection coefficient is positive, and a tensile wave in the bar is reflected as a tensile wave; when $0 < \alpha < 1$, the coefficient is negative and a tensile wave reflects as a compressive wave. With these reflected waves, one would now suspect the emergence of poles in the Green's function, and indeed they do occur, as given by relations (31), (10) and (12).

Relation (52) gives us a way to find the rate of decay/amplification of waves in the bar. Notice that the amplitude of the reflected wave is R times the amplitude of the incoming wave. So it takes a time $\frac{2}{c}$ to change (on average) the amplitude of the original wave by a multiplicative factor of R , and therefore in time t the amplitude of the original wave will get multiplied by $R^{\frac{ct}{2}}$. We note that the exponential term multiplying the amplitude in our solution is $e^{-q_0 ct} = \left(\frac{1-\alpha}{1+\alpha}\right)^{ct/2}$, where we have used relation (10); and this is exactly $R^{\frac{ct}{2}}$ in magnitude! Since at each reflection of the traveling waves from the right hand end of the bar the amplitude gets multiplied by R , the decay (increase) in amplitude will be exponential. And so it will take an *infinite* duration of time for the bar to come to complete rest (or for its amplitude to become unbounded) *unless* $\alpha = 1$ (or $\alpha = -1$).

Observation 7: When $\alpha = 1$, the response caused by a displacement pulse is shown in Fig. 2, indicating that after a time $t \geq \frac{2}{c}$ the response $u(x,t)$ of the system becomes identically zero, and the bar comes to rest in a finite time duration. This behavior has been referred to by Balakrishnan [1] as 'super-stable.'

The response of the system can be easily obtained by realizing that an initial displacement, $f(x)$, splits into two waves, $\frac{1}{2}f(x + ct)$ and $\frac{1}{2}f(x - ct)$; the

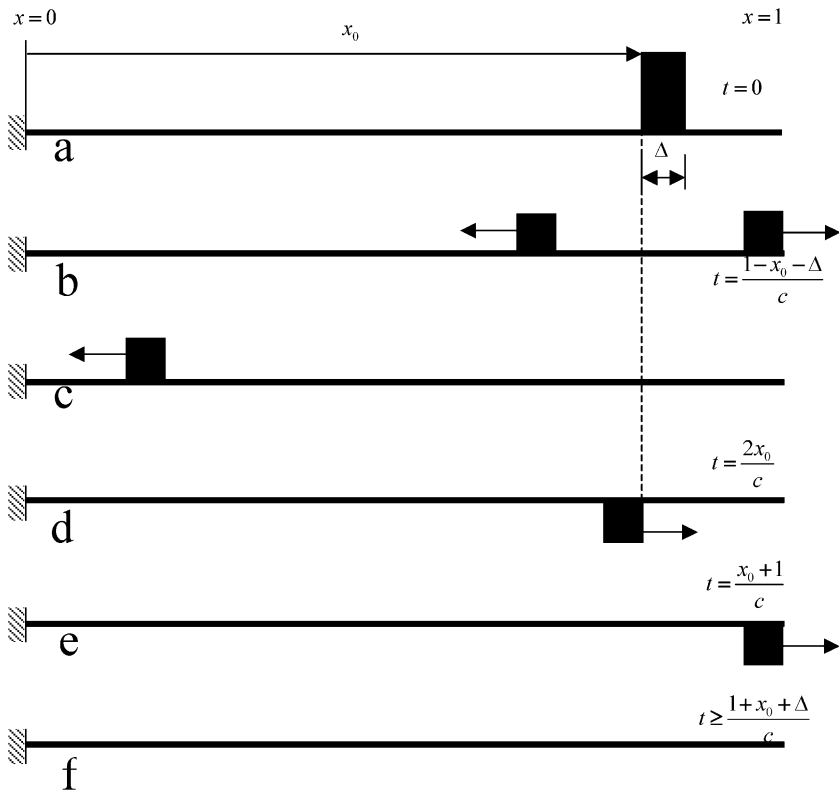


Fig. 2. The response at successive times due to an initial displacement pulse of width Δ applied at $x = x_0$ when $\alpha = 1$. (b) The displacement pulse initially splits into two, each half moving in the two directions. (c) Note the ‘disappearance’ of the rightward moving pulse beyond the right end of the bar. (d) Reflection of the leftward moving pulse shown in (c), from the left hand boundary. (e) Eventual disappearance of this rightward moving pulse also, beyond the right end of the bar. (f) The bar at rest, the pulses having totally exited the bar from its right end.

left-traveling wave reflects off the left-hand boundary at $x = 0$ to give $-\frac{1}{2}f(ct - x)$. These are the three terms that we obtained in relation (35) related to the initial displacement $f(x)$. Similarly to obtain the solution corresponding to an initial velocity, $g(x)$, we know (from D’Alembert’s solution to the wave equation) that integrals of $\frac{1}{2}g(x + ct)$ and $\frac{1}{2}g(x - ct)$ are similarly involved. The last member in the brackets in Eq. (35) gives the reflected waves, caused by reflections of the left-traveling waves off the left boundary where the bar is fixed. As explained in Observation 1, once the rightward traveling waves reach the boundary at $x = 1$, they disappear past it. Consequently, the maximum time for which the response of the system can be nonzero is $2/c$ —twice the time taken for a signal with speed c to traverse the bar.

We have thus physically interpreted Eq. (35) and we observe now that we could have written down the solution (35), which was obtained after considerable labor in the previous section, directly and quite easily by mere inspection!

Assuming that the bar starts with zero initial velocity and with the displacement pulse shown in Fig. 1, changes in its total energy $E(t)$ with time (see Eq. (23)) are shown schematically in Fig. 3. Starting with a total initial energy of E_0 , the energy remains a constant until the rightward traveling pulse reaches the right hand edge, beyond which the pulse disappears, causing the energy to drop to half its starting value at time $(1 + x_0)/c$. After this, the energy remains a constant for the duration of time over which the leftward traveling pulse reflects from the left hand boundary, turns around, and proceeds rightwards until it reaches the right hand boundary. On reaching this boundary, the energy in the bar goes to zero when the pulse moves out of the bar. The system comes to rest after a time $(1 + x_0 + \Delta)/c$. We notice from Fig. 3 that $\dot{E}(t)$ is zero for considerable intervals of time. Hence, viewed as a dynamical system, asymptotic stability *cannot* be deduced directly from Lyapunov’s result by using $E(t)$ as a Lyapunov function; one would need to use something like Lasalle’s or Krasovskii’s Theorem [8,9] to establish asymptotic stability. In fact, we have a much stronger result here: the response goes to zero, not exponentially in time, but after a time $2/c$, which is *finite*.

We note that in a similar manner we can show that the response of the system cannot be identically zero for any time less than $1/c$, for this would be the minimum time required for a pulse starting at the left hand end to ‘fall off’ the

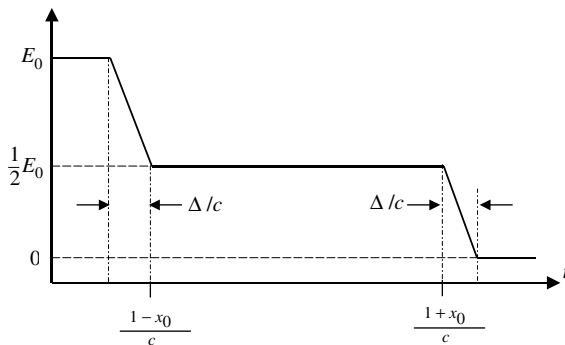


Fig. 3. Schematic plot of the total energy versus time for the displacement pulse shown in Fig. 2. The initial energy in the bar is E_0 and it remains a constant until time $(1 - x_0 - \Delta)/c$ which corresponds to the situation shown in Fig. 2(b). As the rightward traveling pulse moves further, over a time Δ/c , it disappears leaving the bar with just half its initial energy. The energy in the bar remains a constant after that until the pulse upon reflection from the left hand end reaches the right boundary at time $(1 + x_0)/c$ which corresponds to Fig. 2(e). Over the next time interval of Δ/c the pulse leaves the bar, the bar comes to a dead stop, and all the initial energy has been totally drained from it.

right hand end of the bar. Thus when $\alpha = 1$, the minimum time for the system to come to rest is $1/c$; and the maximum time that the system can have a non-zero-response is $2/c$. In other words, when $\alpha = 1$, the system *must* vibrate for all times less than $1/c$, and the system *must* come to rest for all times greater than $2/c$.

Observation 8: For $\alpha < 0$, the absolute value of the reflection coefficient R , from relation (52), exceeds unity and the reflected wave is amplified. For $-1 < \alpha < 0$, R is negative, and for $\alpha < -1$ it is positive. For $\alpha < 0$, energy is now being continually ‘pumped into’ the bar through the right hand boundary at each reflection, and the system’s response will explode exponentially, as we had expected from our arguments in Sections 1 and 2.

Observation 9: When $\alpha = -1$, the reflection coefficient R in relation (52) becomes infinite pointing out that the total wave field $v(x,t)$, of Eq. (50) reaches an infinite amplitude upon reflection. This happens, in our model, as soon as the wave pulse in Fig. 2 reaches the right hand boundary. The amplitude of the system’s response becomes ∞ after time $t \geq \frac{1-x_0-\Delta}{c}$. And so, *an infinite response amplitude is reached in finite time* to an initial displacement—we have a ‘super-unstable’ system! There is thus a similarity in the behavior of our system in this regard with the so-called ‘finite exit-time’ behavior of some non-linear systems, except, of course, that our system is described by a *linear* partial differential equation with *constant* coefficients!

The value of q_0 when $\alpha = -1$ becomes $-\infty$ (see Fig. 1); hence, all the poles, $s_n = -q_0c + ip_{nc}$, move to the right half s -plane and have an abscissa of ∞ . The *maximum* time over which the system’s response could remain finite is then $\frac{1}{c}$; this maximum would occur for a initial displacement pulse located at the left hand end of the bar.

Observation 10: Were the left hand boundary condition to be $c \frac{du(0,t)}{dx} = \frac{du(0,t)}{dt}$, instead of $u(0,t) = 0$, the system discussed above would come to rest for all times $t \geq \max(\frac{x_0+\Delta}{c}, \frac{1-x_0}{c})$. This is an even shorter span of time than $\frac{2}{c}$, since now both boundaries would become quiet; energy would be depleted from both boundaries with no reflections from either of them.

5. Physical description of the boundary conditions and impedance matching

The interesting behavior of the system described by Eqs. (1)–(3) is fundamentally due to the boundary conditions we have imposed. Hence, from a practical viewpoint, the question of whether such boundary conditions, which are modeled by Eq. (2), can be *physically realized* then becomes important [7].

In this section we show that indeed the right hand boundary condition can be handily realized, and, in fact, understanding its physical implementation opens up yet another route to understanding the system’s behavior, this time via the concept of impedance.

The boundary condition at the left hand end of the vibrating bar can be implemented by fixing it, the right hand boundary condition can be realized (for $\eta > 0$) by attaching the right hand end of the bar to a dashpot with damping factor η . This is shown in Fig. 4.

The impedance, I_d , of the dashpot is given by

$$I_d = -\frac{F_d}{\frac{\partial u(1,t)}{\partial t}} = \eta, \tag{53}$$

where F_d is the force in the dashpot. Also, the impedance at $x = 1$ of the bar to an ‘incoming wave,’ given by $v_1(x, t) = A \exp i(kx - \omega t)$ (see Eq. (50)), which travels rightwards in the bar and ‘enters’ the bar’s right hand boundary, is given by

$$I_b = -\frac{F_b}{\frac{\partial v_1(1,t)}{\partial t}} = \frac{EA_0 \frac{\partial v_1(1,t)}{\partial x}}{\frac{\partial v_1(1,t)}{\partial t}} = EA_0 \frac{k}{\omega} = \frac{EA_0}{c}. \tag{54}$$

where, F_b is the force generated in the bar by the incoming wave at $x = 1$.

When the impedance of the incoming wave is exactly matched by the impedance of the dashpot, we have $I_b = I_d$, so that $\eta = \frac{EA_0}{c}$, and $\alpha = 1$ (see the discussion following Eq. (3)). We see that the condition $\alpha = 1$ corresponds to a situation of ‘matched impedances’ at the boundary $x = 1$ and it results in there being no reflection from it. The energy propagating toward the right in the wave that enters the right-hand boundary is completely ‘absorbed’ by the dashpot; we thus see how the energy of vibration leaves the bar at its right-hand end, and ‘disappears’ from it. While the impedance matching concept has been known for some time in application areas such as long transmission lines and acoustics (see for example, Ref. [7]), the explicit solution, as given in Eqs. (43)–(48), of the non-self-adjoint boundary value problem and its mathematical implications appear to have been unavailable so far.

For other values of $\eta > 0$, the impedance of the incoming wave and the impedance of the dashpot are no longer ‘matched,’ and a complete absorption of the energy of the wave that enters the right hand boundary can no longer occur. The boundary then ‘generates’ waves thereby reflecting some of the energy back into the bar. However, since the dashpot absorbs *some* energy (unless $\alpha = 0$ or $\alpha = \infty$) from the incoming wave each time the wave reaches the right hand boundary, the amplitude of the reflected wave is smaller than the

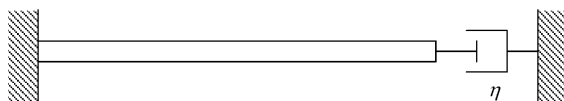


Fig. 4. One possible physical mechanism for generating the boundary conditions given by Eq. (2). At the right hand end is a dashpot. When $\alpha := \frac{EA_0}{c\eta} = 1$, we get the impedance matching condition.

amplitude of the incoming wave, resulting in an exponential amplitude decay of the wave in the bar.

When $\eta < 0$ (that is, when $\alpha < 0$) we can no longer have a ‘passive’ dashpot. We would need an ‘active’ dashpot that inputs energy into the bar, applying a force that is not resistive, but assistive. The right hand boundary condition (2) then becomes less straight-forward to physically realize and implement.

6. Numerical simulations

One way of gaining insight into the behavior of the boundary-controlled system described by Eqs. (1a)–(3a) would be through numerical simulations. In this section we explore some of the computational difficulties in doing this from an analytical viewpoint. We then provide some numerical results that corroborate our understanding of the response of the system.

Our Eqs. (1a)–(3a) are linear, and they describe the bar modeled as a continuum. Any discretization of this system of equations (usually done using finite difference or finite element approaches) would eventually give us a linear, constant coefficient, finite-dimensional system of ordinary differential equations of the form

$$\frac{dw}{dt} = Ww, \quad w(t=0) = w_0, \quad (55)$$

where the number of elements, N , in the column vector, w , depends on the number of mesh points we decide to use in discretizing the spatial domain $(0,1)$, and the N by N square matrix W is a matrix whose elements are *constants* that depend on the specific numerical procedures (and degree of approximations) that we employ in obtaining the finite dimensional approximation (55) to our continuous system.

The poles of our finite-dimensional system (55), in the s -plane are obtained from the roots of the equation

$$\det(W - sI) = 0. \quad (56)$$

By the fundamental theorem of algebra, this N th order polynomial *must* have exactly N *finite* roots (including multiplicities), which are the eigenvalues of the matrix W .

But we found that for $\alpha = 1$ all the poles of our continuous system (1a)–(3a) are in the left half s -plane with their abscissas at $-\infty$! Hence there is no way that the finite dimensional approximation (55) can qualitatively approximate the continuous system *no matter how large we take N to be*.

Alternately stated, when $\alpha = 1$ we know from Section 3 that the continuous system has no finite poles. Every value of s lies in the resolvent set of the second derivative operator described by (25b); its spectrum is empty. Clearly this is

impossible for the finite dimensional matrix approximation, since every N by N matrix W must have N finite eigenvalues.

The physical manifestation of this mathematical result is the following. We see that the general solution to Eq. (55) is

$$w(t) = e^{Wt} w_0,$$

where W is a constant matrix, and no exponential solution can go to zero in finite time! Hence the behavior (for $\alpha = 1$) of our continuous system that comes to a ‘dead stop’ after a time $\frac{2}{c}$ can never be qualitatively mimicked by any discrete approximation, no matter how finely we discretize the spatial domain! This ‘super-stable’ behavior of the continuous system can thus never be *qualitatively* captured by a finite-dimensional approximation. *It is a consequence of the continuum nature of the system described by Eqs. (1a)–(3a).*

Similar arguments can be made for super-unstable behavior, which causes the response of the linear system to become *unbounded in finite time*, when $\alpha = -1$. No system described by the constant coefficient set of linear ordinary differential equations given in Eq. (55) can have an unbounded response in a

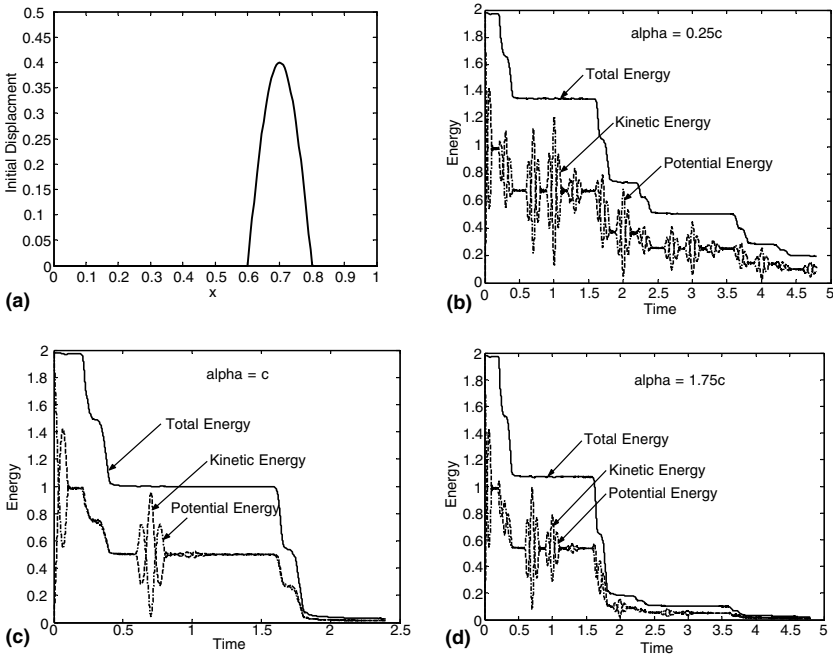


Fig. 5. (a) The initial displacement pulse with zero initial velocity. Comparing with Fig. 2, the location and width of the pulse are $x_0 = 0.6$ and $\Delta = 0.2$ respectively. (b)–(d) Energy response of the system for different values of $\alpha = 0.25, 1,$ and 1.75 .

finite time. Thus super-instability, too, is a consequence of the continuum nature of the partial differential equation model (1a)–(3a), and it cannot be qualitatively captured by any finite N -dimensional approximation, no matter how large N may be.

Having pointed out the difficulty in numerically obtaining a qualitative parity while using a finite-dimensional formulation, we show in Fig. 5(b)–(d) some computed results for an initial displacement pulse (with zero initial velocity)

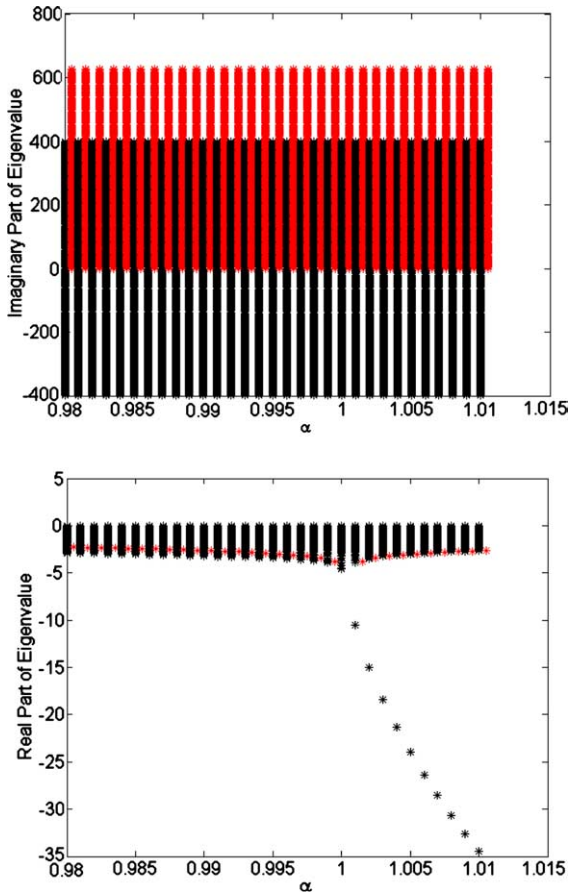


Fig. 6. Eigenvalues of the continuous system and its finite dimensional approximation. The matrix W has dimension 400 by 400. (a) We have shown only those poles of the continuous system with positive imaginary part. The imaginary parts of all poles of the discrete system are shown. For display purposes, the continuum poles are displaced slightly to the right. (b) The real part of the poles of the continuous and discrete system. Notice that all poles of the continuous system have the same real part for any given value of α .

shown in Fig. 5(a). The energy-time plots for $\alpha = 0.25, 1,$ and 1.75 are shown. The value of c is taken to be unity.

The unit length of the continuous bar is discretized using 200 points and the time interval for the integration is taken to be 0.0005 units of time. The results are computed using a finite difference scheme correct to $O(h^2)$. We note that for $\alpha = 1$, the computed results show a small remnant of energy after the time $t = \frac{1+x_0+\Delta}{c} = 1.8$ units, the time after which the continuum should, theoretically, be at rest. This points to the difficulty in qualitatively replicating the behavior of the continuum by using finite dimensional approximations.

Lastly, we show in Fig. 6 the eigenvalues of the matrix W (see of Eq. (55)), the finite dimensional approximation to the partial differential equation system (1a)–(3a) for the range $0.98 \leq \alpha \leq 1.01$. The eigenvalues of the continuum (obtained for Eqs. (31), (10) and (12)) are shown slightly displaced to the right of those obtained for the matrix W ; the latter are obtained by using MATLAB. We observe that for $\alpha \geq 1$, there is a significant deviation of the real parts of the eigenvalues of the continuous system and its finite dimensional approximation. For any given value of α , the real parts of the poles of the continuum model do *not* depend on the mode number while those of the finite dimensional approximation do. The plot also shows the extreme sensitivity of the real part of the eigenvalues of the continuum to the parameter α , which goes to $-\infty$ when $\alpha = 1$.

7. Conclusions

In this paper we study the dynamics of the axial vibrations of a bar subjected to a control force that is proportional to the velocity at its boundary. The bar is initially subjected to a prescribed initial displacement and velocity. The system is not self-adjoint, and we have provided the complete solution of the boundary control problem along with the physical interpretation of when and why the eigenvalues and the eigenfunctions disappear for $\alpha = \pm 1$. We thereby uncover and develop an understanding of the interesting phenomena of super-instability and super-stability. The first causes the system's response to become unbounded in finite time, the second causes the systems response to die down in finite time. Though such behavior (finite exit time) is common in nonlinear systems, we show that its presence in our linear system is intricately related to the continuum modeling of the system. Through the interplay of mathematical analysis, stability theory, and a physical interpretation of the response of the system, we have shown that the behavior of the system has several interesting characteristics. They are as follows:

1. The behavior of the system depends on the value of the parameter that gives the magnitude of the boundary feedback force. When the parameter $\alpha = \pm 1$, we find that the system has *no* eigenvalues and *no* eigenfunctions. Its Green's

function is *entire*. When $\alpha = 1$, the constant coefficient linear system when subjected to an initial displacement and/or velocity comes to rest in *finite* time. We thus explain the presence of such behavior, which has been referred to as super-stable [1].

2. When the parameter $|\alpha| \neq 1$, the Green's function has poles and the system's response can be expressed as a weighted sum of a series of eigenfunctions. Though the system of partial differential equations that describes its response is not self-adjoint, the bar's dynamic behavior can thus still be determined by as an 'expansion' in terms of the eigenfunctions, $u_n(x,t)$. These functions show that the response can be visualized as a sum of exponentially damped traveling waves. The presence of such functions is shown to be tied to the presence of reflections from the boundary of the continuum. Somewhat interestingly, the damping is not dependent on the mode number.
3. Super-stable behavior is explained through the analysis of traveling waves propagating across the medium that produce no reflections at the right hand boundary. This leads to the disappearance of eigenvalues and eigenfunctions; the Green's function becomes entire and all its poles have an abscissa of $-\infty$. We show that this behavior occurs when there is a 'matching' of impedances between the incoming wave and the dashpot at the right-hand boundary of the bar.
4. The analysis also shows the presence of 'super-unstable' behavior when $\alpha = -1$. The response of the linear system goes to infinity in *finite* time. Again the system has no eigenvalues or eigenfunctions, and the real part of every pole of the Green's function of the system now has an abscissa of ∞ .
5. It is shown that no finite dimensional model obtained through spatial discretization, no matter how fine, can qualitatively capture the super-unstable or super-stable behavior of this continuous system. These properties appear to be *intrinsic* to the continuum nature of the model that we describe here through the use of partial differential equations.

The governing equations that we have used to describe the system arise in numerous fields like structural dynamics, structural control, earthquake engineering, and computational mechanics, and it is hoped that these results will shed light in these and other application areas where they arise. Though the impedance concept has been long utilized in acoustics and waves in transmission lines, the explicit solution of the non-self-adjoint problem and its physical and mathematical implications related to super-stability and super-instability do not appear to have been available to date.

Acknowledgement

The author is grateful to Prof. A.V. Balakrishnan at UCLA for his presentation at the 12th International Workshop on Dynamics and Control, August

19–21, 2002, which triggered the author's interest. He is thankful to Professor Balakrishnan for discussions and his comments.

References

- [1] A.V. Balakrishnan, Superstability: Theory and Experiment, in: 12th International Workshop on Dynamics and Control, August 19–21, 2002.
- [2] J.L. Lions, Exact controllability, stabilization and perturbations for distributed systems, *SIAM Rev.* 30 (1) (1988).
- [3] J.L. Lions, *Optimal Control of Systems Governed by Partial Differential Equations*, Springer-Verlag, 1971.
- [4] A. Barclay, P.E. Gill, J.B. Rosen, SQP methods and their applications to numerical optimal control, in: W.H. Schmidt, K. Heier, L. Bittner, R. Bulirsch (Eds.), *Variational Calculus, Optimal Control and Applications*, vol. 124, Int. Series Numer. Mathematics, Basel, Birkhäuser, 1998, pp. 207–222.
- [5] R. Datko, Applications of the finite laplace transform to linear control problems, *SIAM J. Contr. Optim.* 18 (1) (1980) 1–20.
- [6] G. Chen G, A note on the boundary stabilization of the wave equation, *SIAM J. Contr. Optim.* 19 (1) (1981) 106–113.
- [7] L. Brekhovskikh, V. Goncharov, *Mechanics of Continua and Wave Dynamics*, Springer-Verlag, 1984.
- [8] N.N. Krasovskii, *Certain Problems in the Theory of Stability*, Mir Publication, 1968.
- [9] J. Lasalle, S. Lefschetz, *Stability by Liapunov's Direct Method with Applications*, Academic Press, New York, 1961.